# Cytomegalic inclusion disease: intrauterine sonographic diagnosis using findings involving the brain.

G B Tassin, N F Maklad, R R Stewart and M E Bell

*AJNR Am J Neuroradiol* 1991, 12 (1) 117-122
http://www.ajnr.org/content/12/1/117

# Cytomegalic Inclusion Disease:
## Intrauterine Sonographic Diagnosis Using Findings Involving the Brain

Gerard B. Tassin[1,2]
Nabil F. Maklad[1]
Rhonda R. Stewart[1,3]
Margaret E. Bell[4]

**Two second-trimester cases and one third-trimester case of intrauterine cytomegalic inclusion disease (CID) are presented, each having a different intracranial sonographic presentation. The findings are correlated with radiographic studies and the known pathophysiology. Sonographic evidence of intrauterine cerebral necrosis or calcification should alert one to the possibility of CID, particularly if other signs of in utero infection are present. A pattern of bilateral periventricular calcifications, which may be preceded by hypoechoic periventricular ringlike zones, seems to be specific for intrauterine CID. However, CID also may result in widespread cerebral destruction. If the sonographic study produces an uncertain diagnosis, sonography can still aid in the prenatal diagnosis of CID by guiding percutaneous umbilical cord blood sampling for serology or by directing amniocentesis for cytomegalovirus culture.**

**The ability of sonography to demonstrate specific characteristics of CID in utero enables prenatal diagnosis of this disease.**

***AJNR* 12:117–122, January/February 1991**

Cytomegalovirus (CMV) is a ubiquitous DNA virus belonging to the herpesvirus family. It is the most frequent cause of fetal and neonatal viral infection [1]. Intrauterine acquisition of infection, presumably through transplacental transmission of virus, can occur secondary to recurrent or primary maternal infection. Reactivation of latent maternal infection is associated with a 3.4% prevalence of congenital fetal infection [2]. Such an infected neonate is usually asymptomatic but does run a risk of developing long-term neurologic sequelae [3]. In contrast, primary CMV infection during pregnancy poses a 30–50% risk of intrauterine transmission and a 21% chance of a symptomatic infected infant [4, 5]. Clinical findings of the classic fetal cytomegalic inclusion disease (CID) syndrome consist of hemolytic anemia with hyperbilirubinemia and jaundice; thrombocytopenia with petechiae or purpura; hepatosplenomegaly; pneumonitis; and CNS abnormalities such as microcephaly, ocular defects, and deafness [6].

Few radiologic references address the prenatal diagnosis of CID and still fewer mention the intrauterine CNS findings [7–11]. We report a series of three cases of intrauterine CID, demonstrating a spectrum of intracranial findings. The unique role of sonography in the prenatal diagnosis of CID is addressed.

### Case Reports

*Case 1*

A 20-year-old white woman, G3P0112, with a 25-week gestational intrauterine pregnancy was transferred to our institution 5 days following premature rupture of membranes. Sonographic evaluation in our department revealed a single viable fetus. The biparietal diameter and head circumference were both decreased relative to estimated gestational age, measuring 51.0 mm (21.5 ± 2 weeks) and 210.9 mm (23.2 ± 2 weeks), respectively. Abdominal

Received February 22, 1990; revision requested June 7, 1990; revision received August 21, 1990; accepted August 28, 1990.

[1] Department of Diagnostic Radiology, The University of Texas Health Science Center, 6431 Fannin, Houston, TX 77030. Address reprint requests to N. F. Maklad.

[2] Present address: Department of Diagnostic Radiology, Box 57, The University of Texas M. D. Anderson Cancer Center, 1515 Holcombe Blvd., Houston, TX 77030.

[3] Present address: Department of Radiology, The Alexandria Hospital, 4320 Seminary Rd., Alexandria, VA 22304.

[4] Department of Pathology, The University of Texas Health Science Center, Houston, TX 77030.

0195-6108/91/1201-0117

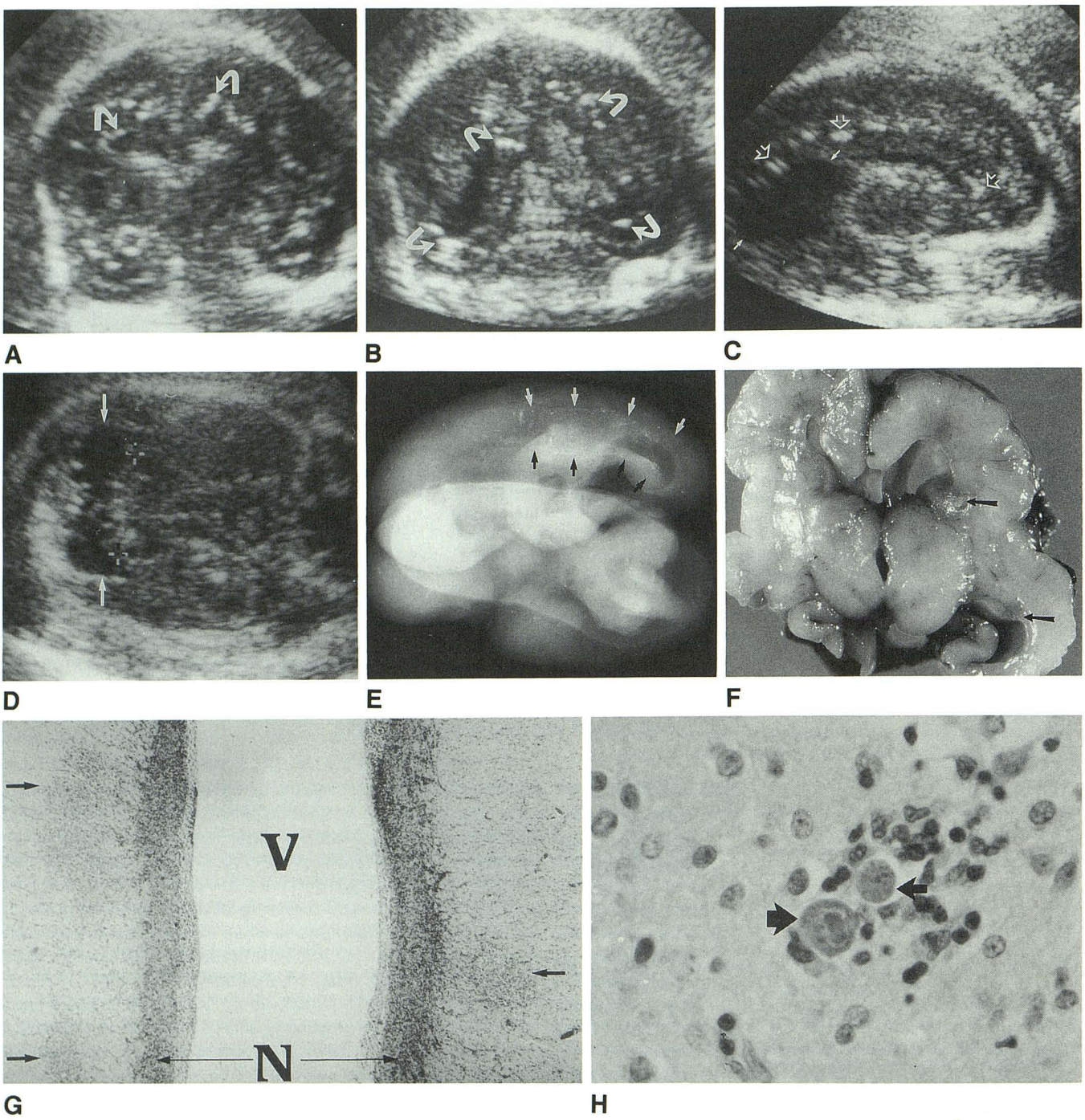


Fig. 1.—Case 1: Bilateral periventricular calcifications in a fetus.

*A* and *B*, Antenatal coronal sonograms of a 25-week-gestation brain at level of frontal horns (*A*) and atria (*B*) of lateral ventricles reveal multiple bilateral hyperechoic foci (*arrows*) consistent with calcifications.

*C*, Parasagittal scan of fetal brain shows calcifications (*open arrows*) extending posteriorly in a periventricular distribution. Note hypoechoic structure in posterior fossa (*solid arrows*).

*D*, Axial sonogram of brain at level of cerebellum (*between cursors*) again shows that hypoechoic posterior fossa structure (*arrows*) is not insinuating itself between cerebellar hemispheres. Transverse cerebellar diameter measures approximately 19.4 mm (<10th percentile). Autopsy showed no evidence of a posterior fossa cystic lesion but did demonstrate a small, immature cerebellum with dystrophic calcification, thus accounting for compensatory expansion of adjacent subarachnoid space.

*E*, Radiograph of fetal brain after fixation and removal of dura shows extensive parenchymal calcification surrounding ventricles (*arrows*).

*F*, Coronal section of brain at level of thalamus and hippocampus reveals focal regions of subependymal necrosis with macroscopic dystrophic calcification (*arrows*) around body and temporal horns of lateral ventricle.

*G*, Microscopic section through frontal lobe shows foci of necrosis with mineralization (*arrows*) in subependymal germinal matrix, into which migrating neuroblasts (N) have sent numerous cytoplasmic processes. V = ventricular lumen. (H and E, ×100)

*H*, Classic cytomegalovirus cell (*large arrow*) demonstrates large intranuclear inclusion with a variable number of small intracytoplasmic inclusions. A second cytomegalovirus cell (*smaller arrow*) is present but nucleus is out of plane of section; therefore, only intracytoplasmic inclusions are seen in the second cell. (H and E, ×400)

circumference was 210.4 mm (25.6 ± 2 weeks) and the head circumference/abdominal circumference ratio was 1.00 (normal, 1.03–1.22). Extensive areas of periventricular calcification were noted within the brain (Figs. 1A and 1B). A posterior fossa hypoechoic structure was believed to represent prominence of the cisterna magna (Figs. 1C and D). Oligohydramnios was present.

On the basis of sonographic findings, a diagnosis of intrauterine CID was made. The patient elected to terminate the pregnancy, delivering a 720-g stillborn girl. CMV immunoglobulin G immunofluorescent antibody titer (IFAT) on cord serum was positive at a titer of ≥1:640 (normal, <1:5). CMV immunoglobulin M IFAT was positive at ≥1:10 (normal, <1:10).

Fetal necropsy showed a cranial circumference of 21 cm (10th percentile) and a brain weight of 69.1 g (<10th percentile). A specimen radiograph of the brain showed the extent of the parenchymal calcification (Fig. 1E). Gross brain sections demonstrated periventricular necrosis and mineralization inclusive of the fourth ventricle and occipital horns of the lateral ventricles (Fig. 1F). Microscopic examination confirmed the gross findings and, in addition, revealed the histologically characteristic inclusion-bearing cells of CID (Figs. 1G and 1H). Inclusion-bearing cells were also isolated from the lung, liver, pancreas, kidney, adrenals, and thyroid.

Postmortem viral cultures were positive for CMV in the brain, lung, liver, kidney, placenta, and umbilical cord. Microbiology for coexisting congenital toxoplasmosis was negative. Viral cultures from the mother were positive for CMV in the cervical secretions but not in the urine.

*Case 2*

A 26-year-old G1P000 black woman was referred to our department at 25-weeks gestation for evaluation of suspected fetal hydrocephalus in an otherwise uncomplicated pregnancy. The initial sonographic examination at our institution demonstrated mild to moderate hydrocephalus. The biparietal diameter measured 5.7 cm (24.5 ± 2 weeks). Multiple scan planes of the fetal head revealed bilateral periventricular hypoechoic areas, each in the configuration of a ring (Figs. 2A and 2B). Serial sonographic examinations at 28, 30, 32, 36, and 40 weeks of gestation revealed mild progressive ventricular

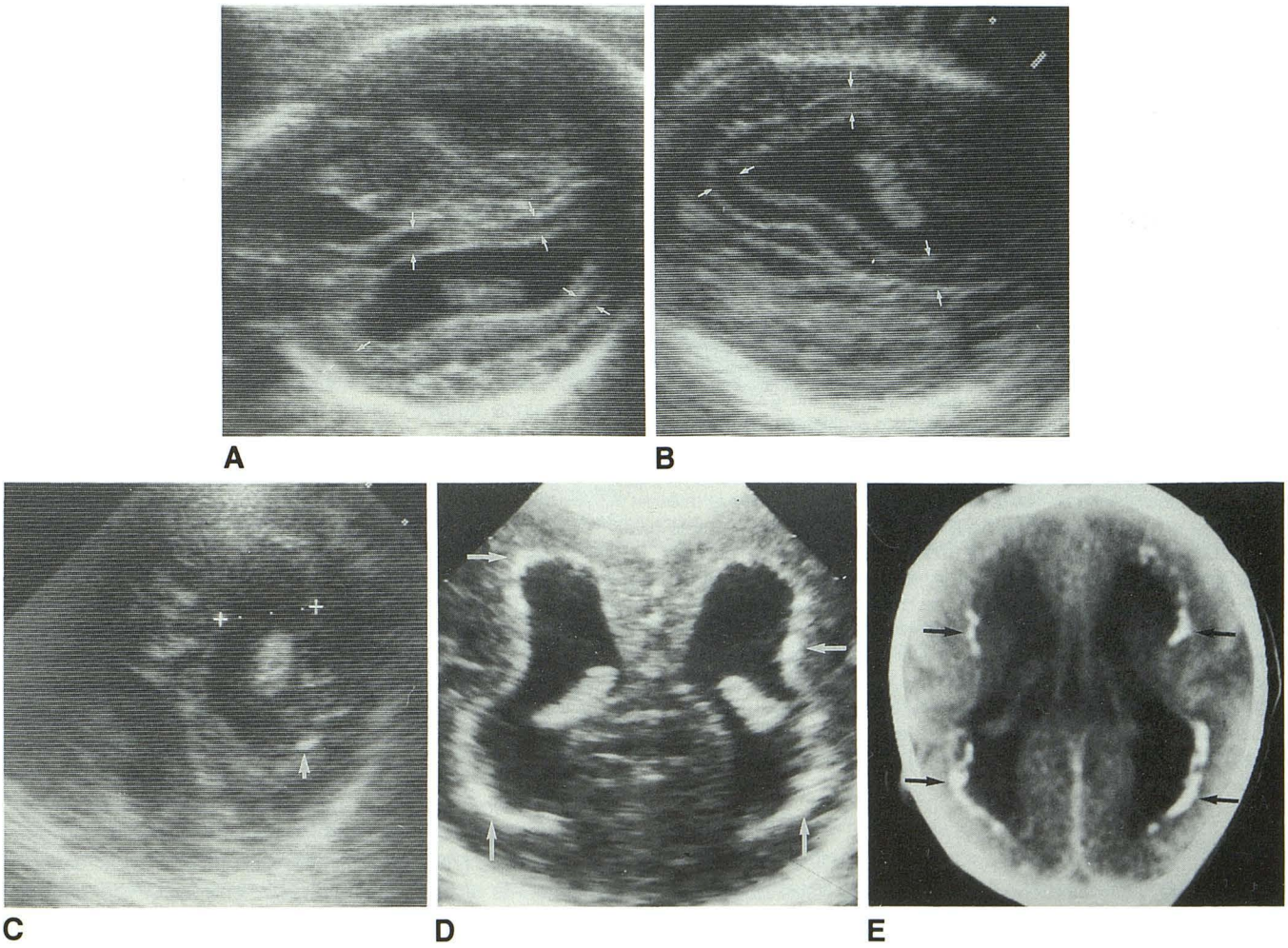


**Fig. 2.—Case 2: Hypoechoic periventricular rings preceding development of periventricular calcifications.**

***A* and *B*, Axial (*A*) and oblique sagittal (*B*) antenatal sonograms of a fetal brain at 25 gestational weeks show moderate ventriculomegaly with bilateral hypoechoic periventricular ringed zone (*arrows*). Reverberation artifact from near calvarial wall largely obscures proximal cerebral hemisphere on axial scan.**

***C*, Coronal sonogram of fetal brain at 36-weeks gestation reveals persistent ventriculomegaly with an atrial width (*cursors*) of 1.8 cm. Hypoechoic periventricular rings are no longer apparent. Calcifications are now seen in subependymal regions (*arrow*).**

***D* and *E*, Initial neonatal brain sonogram (*A*) and axial CT scan (*B*) on the first day of life show progression of calcification (*arrows*) surrounding enlarged ventricles since last prenatal study.**

enlargement. At 28 weeks, the periventricular hypoechoic areas had been largely replaced by mildly hyperechoic brain parenchyma. By 36 weeks, periventricular calcification was unequivocal (Fig. 2C). The ratio of head circumference, 28.88 cm (31.5 weeks), to abdominal circumference, 30.62 cm (35 weeks), was 0.94 (fifth percentile). At 40 weeks, the biparietal diameter was 8.2 cm, more than 3 SD below the mean for gestational age.

At 41-weeks gestation, the patient delivered a microcephalic 3420-g (50th percentile) male infant. The cranial circumference measured 31.5 cm (<10th percentile). Brain sonography and CT on the first day of life showed extensive periventricular calcifications with moderate ventricular dilatation (Figs. 2D and 2E).

CMV immunoglobulin G IFAT of the mother's and infant's serum was positive at a titer of 1:1024. CMV was subsequently isolated from the infant's urine. Maternal and fetal toxoplasmosis immunoglobulin G IFAT were negative.

*Case 3*

A 22-year-old white woman, G3P0020, was transferred to our institution at 29.5 gestational weeks with a diagnosis of preeclampsia (blood pressure, 160/110 mm Hg) and multiple fetal anomalies. On admission, the patient's blood pressure was normal and stable. Sonographic examination revealed a single intrauterine fetus with abdominal ascites, hepatomegaly, and a pericardial effusion. The left half of the intracranial space was anechoic; the right half was a disorganized mass of mixed echogenicity with scattered calcifications (Fig. 3A). Except for a few ossified segments, the calvarial mineralization was grossly deficient. The bony facial structures also were not seen well. Although the head circumference measured 316.3 mm (35.5 ± 3 weeks), the femur length was only 45.2 mm (24.9 ± 2 weeks). Oligohydramnios and placentomegaly were present (Fig. 3B).

Following the patient's decision to terminate the pregnancy, cephalocentesis was performed and 130 ml of bloody CSF was aspirated. A 1485-g stillborn boy was subsequently delivered. Grossly, there was proptosis of the left eye, a small mouth, and low-set ears. Postmortem radiographs demonstrated poor ossification of the calvaria and distortion of the facial skeleton (Fig. 3C). Necropsy revealed diffuse serosal petechial hemorrhages, hepatosplenomegaly, and generalized fetal hydrops. The brain was extensively distorted with a large area of hemorrhage essentially replacing the left parietal and temporal lobes (Fig. 3D). Extensive necrosis with both fresh and old blood constituted the right cerebral hemisphere, extending from the ependyma of the lateral ventricle to the cerebrum with calcification, ependymal erosions, and glial aggregates (Fig. 3E). Vascular proliferation was present at the margins of this necrotic mass in an attempt at organization. The placenta measured 18 × 16 × 3 cm and weighed 800 g; widespread areas of villous edema were noted (Fig. 3F). Cytomegalic inclusion-bearing cells were seen in the lungs and pancreas. Chromosomal analysis was normal (46,XY).

## Discussion

Congenital CMV infection has traditionally been diagnosed in the neonate via one of the following: (1) positive CMV culture of body fluids, (2) the presence of CMV-specific immunoglobulin M titers in the infant's serum, or (3) demonstration of large intranuclear inclusions with small variable intracytoplasmic inclusions in CMV-infected visceral cells. Sonography has provided a means by which CID can be diagnosed prenatally. There are only two prior reports of the prenatal sonographic demonstration of bilateral periventricular calcifications [7, 8]. This particular intrauterine distribution is virtually specific for CID, although other infectious agents may cause periventricular calcifications in an infant. Routine radiography has documented periventricular calcifications in infants with toxoplasmosis [12] and with bacterial meningitis complicated by ventriculitis [13], but to our knowledge, no particular sonographic CNS manifestation has been described prenatally in either of these two entities. Bacterial meningitis is not a diagnostic consideration in a fetus. Additionally, histologic correlation has shown that the calcifications in neonatal toxoplasmosis are not primarily subependymal but are widely distributed in necrotic brain tissue or, uncommonly, have a characteristic curvilinear pattern in the basal ganglia [12]. Thus, it seems likely that sonography, given its sharp delineation of ventricular margins, would be more specific than skull radiography in differentiating between the intracranial calcifications of toxoplasmosis and those of CID. The remaining infections of the TORCH (toxoplasmosis, rubella, CMV, and herpes simplex virus) family—rubella virus and herpes simplex virus—have not been shown conclusively to cause a bilateral periventricular pattern of macroscopic calcifications in either the fetus or the neonate, although herpes simplex virus infection in an infant has rarely been associated with cerebral calcification on skull radiography [14, 15]. Noninfectious causes of bilateral periventricular calcification are essentially limited to tuberous sclerosis, which presents no diagnostic difficulty as the subependymal nodules do not calcify until childhood.

Ringlike areas of periventricular lucency, as found in our second case, are a previously unreported finding in congenital CID and may represent the earliest sonographically demonstrable abnormality prior to the development of subependymal calcifications. The exact cause of these lucent zones is unknown since autopsy proof was not available in this case. However, on the basis of the known pathophysiology of CID, the hypoechoic areas may be related to cellular necrosis with inflammatory edema and/or local blood effusion. In the fetus, CMV has a special affinity for the metabolically active neuroblasts of the subependymal matrix. In addition, inclusion bodies are often found in the endothelial lining of subependymal blood vessels, and a mononuclear perivascular infiltrate is invariably present [16]. Either as a result of a direct cytopathic of CMV on the neuroblasts and/or on the regional vasculature, subependymal degeneration results. The accompanying inflammation can be expected to result in localized edema and the vascular alterations are manifested by a subependymal blood effusion [16]. As a consequence of the CMV infection, the fetus is expected to be anemic, as verified by the presence of nucleated RBCs in the peripheral circulation (Fig. 3F). Thus, this combination of fluid with relatively low amounts of protein would result in a hypoechoic subependymal zone on sonography. If this is the case, Figures 2A and 2B are, therefore, snapshots of the CMV encephalic lesion in evolution. The effusion is cleared later by the reticuloendothelial system and replaced with glial scarring and dystrophic calcification, giving the typical pattern of bilateral periventricular calcifications.

Depending on several factors, including gestational age at the time of infection and virulence of the infection, other

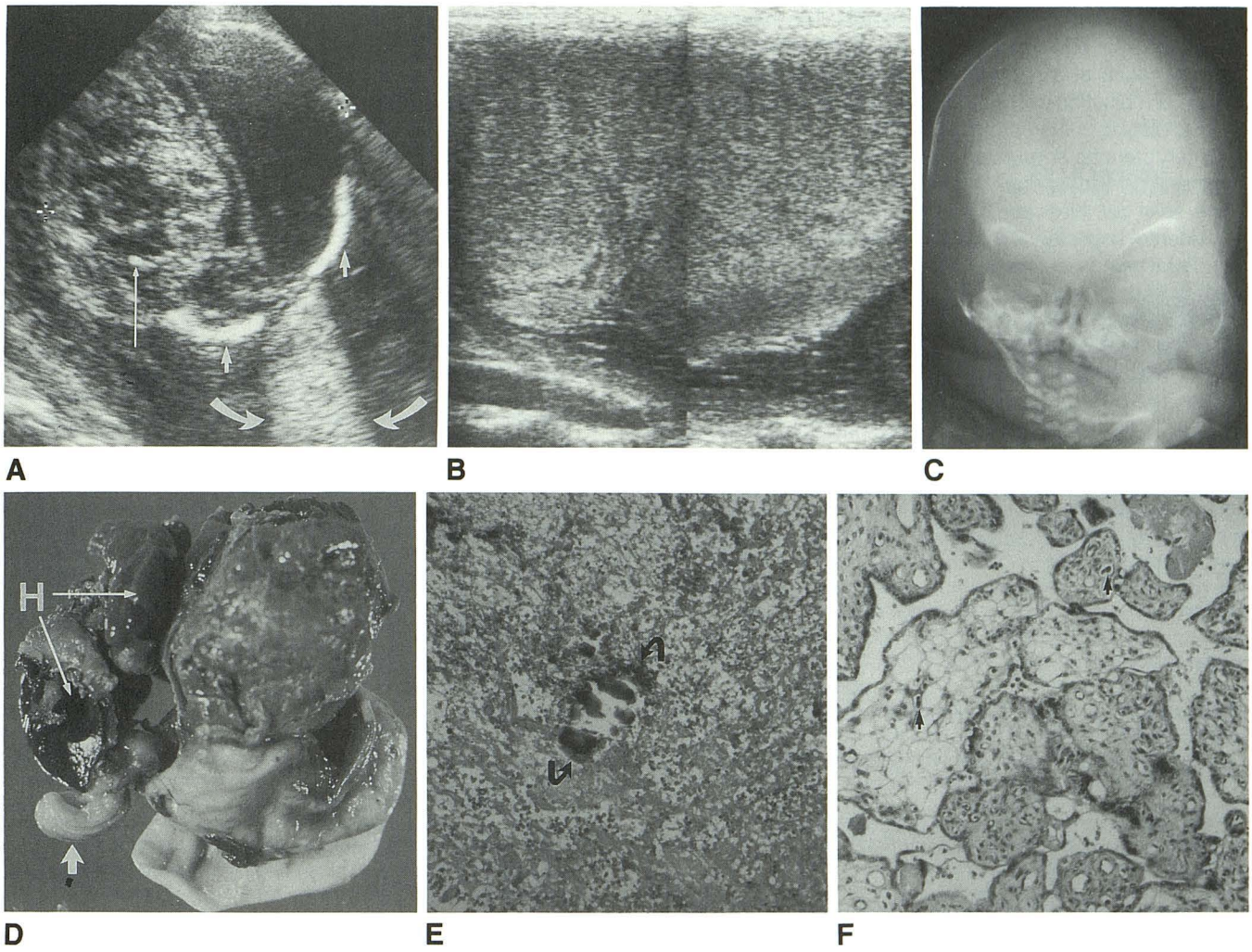


**Fig. 3.—Case 3: Severe distortion of cerebral architecture.**

***A*, Axial sonogram of fetal brain shows fluid in left intracranial space. Note increased sound transmission (*curved arrows*) posterior to left half of head as sound beam exits between two ossified portions of skull (*short straight arrows*). Right cerebral hemisphere is a distorted mass of mixed echogenicity containing a few foci of calcification (*long straight arrow*). Biparietal diameter (*cursors*) measures 95.2 mm (38.8 ± 3 weeks).**

***B*, Composite image of placenta with linear-array transducer shows generalized decreased echogenicity. Placenta measured 13.8 cm in vertical height and extended nearly the length of the uterus.**

***C*, Anteroposterior radiograph of fetal head following cephalocentesis and delivery shows distortion of facial skeleton and enlargement of left orbit. Calvaria is enlarged and poorly ossified.**

***D*, Photograph of posterior aspect of brain after fixation and removal from skull shows severe distortion of cerebral architecture with extensive necrosis of right cerebral hemisphere. Old hemorrhage (H) occupies most of left intracranial space. A portion of cerebellum (*arrow*) is relatively intact.**

***E*, Microscopic section shows focus of calcification (*arrows*) in necrotic brain. (H and E, ×250)**

***F*, Widespread areas of edematous villi with dilated blood vessels are present in placenta, adjacent to otherwise normal third-trimester villi. Nucleated hematopoietic elements (*arrows*), including many nucleated RBCs, are seen throughout placental vasculature, consistent with fetal infection. (H and E ×250)**

cerebral abnormalities may occur via a similar mechanism. For example, in infants with CMV infection, other investigators have found focal paraventricular cysts with or without periventricular calcifications [17, 18]. These paraventricular cysts have been shown to result from focal subependymal necrosis and glial reaction as a consequence of the special affinity of CMV for the actively replicating cells of the richly vascularized subependymal matrix [19]. We found no subependymal cysts in our fetuses.

Alternatively, some have proposed a process of postmigratory ischemic necrosis to account for CMV-induced cerebral damage [20, 21]. The subependyma of the fetal brain, being highly susceptible to ischemia, could theoretically necrose and later calcify. Indeed, other ischemic destructive lesions, such as porencephaly, hydranencephaly, and polymicrogyria, have been associated with CID [20, 21]. The mechanism of the proposed transient fetal ischemia is unclear but may be related to CMV placentitis. Although there are relatively few published observations on the placenta in CID, in cases of overt infection certain histopathologic findings have been observed, the most consistent of which are congestion and edema of the chorionic villi [22, 23]. Figure 3B is the sono-

graphic equivalent of this CMV placentitis. The inherent functional ischemia of a macroplacenta is well known. Thus, the demonstration of a hypoechoic macroplacenta on sonography, in combination with intracranial calcifications, should alert the radiologist to the possibility of CID.

When prenatal sonography demonstrates cerebral abnormalities in the absence of bilateral periventricular calcifications, as in our third case, the diagnosis of CID should still be considered, especially if additional signs of infection are present. Fetal ventriculomegaly, brain atrophy, prominence of the subarachnoid space, and microcephaly have all been documented prenatally in CID [9, 10]. Non-CNS signs of infection reported prenatally in CID include intrauterine growth retardation, hepatosplenomegaly, and ascites [10, 11, 24]. If any of the prior findings are sonographically evident, sonography can futher aid in the in utero detection of CID by providing an invasive role via (1) guidance of percutaneous umbilical cord blood sampling for isolation of fetal CMV-specific immunoglobulin M after 18–20 gestational weeks [24] or (2) guidance of amniocentesis for isolation of CMV from amniotic fluid cultures [25].

## REFERENCES


1. Panjvani ZFK, Hanshaw JB. Cytomegalovirus in the perinatal period. *Am J Dis Child* **1981**;135:56–60
2. Stagno S, Reynolds DW, Huang ES, Thames S, Smith R, Alford C Jr. Congenital cytomegalovirus infection: occurrence in an immune population. *N Engl J Med* **1977**;296:1254
3. Peckham CS, Chin KS, Coleman JC, Henderson K, Hurley R, Preece PM. Cytomegalovirus infection in pregnancy: preliminary findings from a prospective study. *Lancet* **1983**;1:1352
4. Stagno S, Pass RF, Dworsky ME, et al. Congenital cytomegalovirus infection. The relative importance of primary and recurrent maternal infection. *N Engl J Med* **1982**;306:945–949
5. Stagno S, Pass RF, Cloud G, et al. Primary cytomegalovirus infection in pregnancy. Incidence, transmission to fetus, and clinical outcome. *JAMA* **1986**;256:1904–1908
6. Hanshaw JB, Dudgeon JA, Marshall WC. *Viral diseases of the fetus and newborn*, 2nd ed. Philadelphia: Saunders, **1985**:92–131
7. Graham D, Guide SM, Saunders RC. Sonographic features of in utero periventricular calcification due to cytomegalovirus infection. *J Ultrasound Med* **1982**;1:171–172
8. Ghidini A, Sirtori M, Vergani P, Mariani S, Tucci E, Scola GC. Fetal intracranial calcifications. *Am J Obstet Gynecol* **1989**;160:86–87
9. Mittelmann-Handwerker S, Pardes JG, Post RC, Sumala M, Rosenberg JC, Chervenak FA. Fetal ventriculomegaly and brain atrophy in a woman with intrauterine cytomegalovirus infection. *J Reprod Med* **1986**;31:1061–1064
10. Eliezer S, Ester F, Ehud W, Henryk Z. Fetal splenomegaly, ultrasound diagnosis of cytomegalovirus infection: a case report. *JCU* **1984**;12:520–521
11. Price JM, Fisch AE, Jacobson J. Ultrasonic findings in fetal cytomegalovirus infection. *JCU* **1978**;6:268
12. Dyke CG, Wolf A, Cowen D, Paige BH, Caffey J. Toxoplasmic encephalomyelitis. *AJR* **1942**;47:830–844
13. Kotagel S, Tantanasirivongse S, Archer CR. Periventricular calcification following neonatal ventriculitis. *J Comput Assist Tomogr* **1981**;5:651–653
14. South MA, Tompkins WAF, Morris CR, Rawls WE. Congenital malformation of the central nervous system associated with genital type (type 2) herpesvirus. *J Pediatr* **1969**;75:13–18
15. Schaffer AJ. *Diseases of the newborn*, 2nd ed. Philadelphia, Saunders, **1965**:733–734
16. Courville CB. Cerebral lesions in cytomegalic inclusion disease. *Bull Los Angeles Neurol Soc* **1961**;26:9–22
17. Shackelford GD, Fulling KH, Glasies CM. Cysts of the subependymal germinal matrix: sonographic demonstration with pathologic correlation. *Radiology* **1983**;149:117–121
18. Butt W, Mackay RJ, de Crespigmy LC, Murton LJ, Ray RND. Intracranial lesions of congenital cytomegalovirus infection detected by ultrasound scanning. *Pediatrics* **1984**;73:611–614
19. Shaw CM, Alvord EC. Subependymal germinolysis. *Arch Neurol* **1974**;31:374–381
20. Dias MJM, van Rijckevorsel GH, Landriue P, Lyon G. Prenatal cytomegalovirus disease and cerebral microgyria: evidence for perfusion failure, not disturbance of histogenesis, as the major cause of fetal cytomegalovirus encephalopathy. *Neuropediatrics* **1984**;15:18–24
21. Friede RL, Mikolasek J. Postencephalic porencephaly, hydranencephaly or polymicrogyria. A review. *Acta Neuropathol* (Berlin) **1978**;43:161–168
22. Monif GRG, Dische RM. Viral placentitis in congenital cytomegalovirus infection. *Am J Clin Pathol* **1972**;58:445–449
23. Benirschke K, Mendoza GR, Bazeley PL. Placental and fetal manifestations of cytomegalovirus infection. *Virchows Arch [B]* **1974**;16:121–139
24. Lange I, Rodeck CH, Morgan-Capner P, Simmons A. Prenatal serological diagnosis of intrauterine cytomegalovirus infection. *Br Med J* **1982**;284:1673–1674
25. Huikeshoven FJ, Wallenburg HC, Jahoda MG. Diagnosis of severe fetal cytomegalovirus infection from amniotic fluid in the third trimester of pregnancy. *Am J Obstet Gynecol* **1982**;142:1053–1054